



Alkali metal atomic transition probability in strong external magnetic field and its application

C. Leroy¹, G. Hakhumyan^{1,2}, Y. Pashayan-Leroy¹, D. Sarkisyan²

¹Laboratoire Interdisciplinaire Carnot de Bourgogne, UMR CNRS 5209 - Université de Bourgogne, F-21078 Dijon Cedex, France

²Institute for Physical Research, NAS of Armenia, Ashtarak, 0203, Armenia

ABSTRACT

Interaction of alkali atoms with external magnetic field induced a splitting and a shift of their energy levels. We have study this interaction for external field from 0 to 5000 Gauss when the alkali vapor is confined in submicron thin vapor cell with thickness $L = \lambda/2$. Rubidium and Sodium vapors have been studied. The Hamiltonian can be expressed as the sum of the unperturbed atomic Hamiltonian and the so-called Zeeman Hamiltonian. The probability of a transition, induced by the laser electric field is proportional to the square of the transfer coefficients modified by the presence of the magnetic field. We will show that the strong nonlinearity of the transition intensities versus the external magnetic field intensity is obvious for $B > 100$ G. Some possible application for Laser Spectroscopy of the Rb and the Na atoms are presented

Keywords: Zeeman Hamiltonian, atomic transition intensity, frequency shift, submicron thin vapor.

1. INTRODUCTION

Optical nano-cells (NCs) containing atomic vapor of alkali metal have already proved their efficiency to study atomic phenomena with a precision that normal size cells cannot achieve. One could even define as elegant tool such a device when used for the interpretation of interaction between atom and light, atom and surface or atom and atom¹⁻⁸.

A NC has one of his dimensions L of nanometric thickness, that is, L can vary continuously from 0.1 to 10λ where λ is the laser wavelength resonant with the considered atomic transition while the two others dimensions are of centimeter order.

Furthermore, one of the main advantages of this elegant tool appears when one considers the atomic transitions of alkali atoms in magnetic fields. Indeed, for centimeter size thickness cell, the splitting of these transitions into their Zeeman components is relatively bad resolved due mainly to Doppler broadening and the resolution becomes even worst when the external magnetic field increases: well-known saturation absorption method allows only studying the behaviour of a total set of hyperfine transitions and becomes useless for magnetic field such that $B > 100$ G if one wants to describe individual hyperfine transition.

The high resolution atomic spectra obtained with NCs come from the possibility to highly reduce the Doppler broadening. This may be seen if one examines the efficiency of the optical pumping which is given by the following coefficient

$$\eta \sim \frac{\Omega^2 \gamma_N t}{(\Delta + \vec{k} \cdot \vec{v})^2 + \Gamma^2} \quad (1)$$

where t is the time of interaction of the radiation with the atom, Δ is the detuning of the resonance, Γ is the sum of homogeneous and non-homogeneous broadenings, γ_N is the spontaneous decay of the considered transition, Ω is the Rabi frequency of the laser radiation which direction of propagation is \vec{k} and \vec{v} is the atomic velocity.

An obvious way to increase the coefficient (1) is to be as close as possible to the resonance ($\Delta \sim 0$) and to perform a spectrum such that the experimental condition $\vec{k} \cdot \vec{v} = 0$ is fulfilled. NC is an elegant and powerful device that realizes this condition: for the atoms flying perpendicularly to the laser beam the interaction time is $t_{\perp} = \frac{D}{v}$, where D is the diameter of the laser beam, while for the atoms flying parallel to the laser beam, the

interaction time is $t_{\parallel} = \frac{L}{v}$. Thus, with a laser beam of diameter $D \sim 1$ mm and distance between the walls of the $NC L \sim 10^2 - 10^3$ nm, t_{\perp} is 3 to 4 orders higher than t_{\parallel} . Moreover the atoms which fly perpendicularly to the laser beam verify the condition $\vec{k} \cdot \vec{v} = 0$ and expression (1) takes the maximum value at $\Delta = 0$, the VSOP peaks are exactly at the atomic transition frequencies.

To demonstrate briefly the efficiency of the use of NCs to reduce the Doppler broadening, we show on Fig. 1 and 2 (respectively) the spectra for ordinary cell and NC (respectively) for the transition of ^{87}Rb $F_g = 1 \rightarrow F_e = 0, 1, 2$ and for the transition of ^{87}Rb $F_g = 1 \rightarrow F_e = 1, 2$; ^{85}Rb $F_g = 2 \rightarrow F_e = 2, 3$ (respectively).

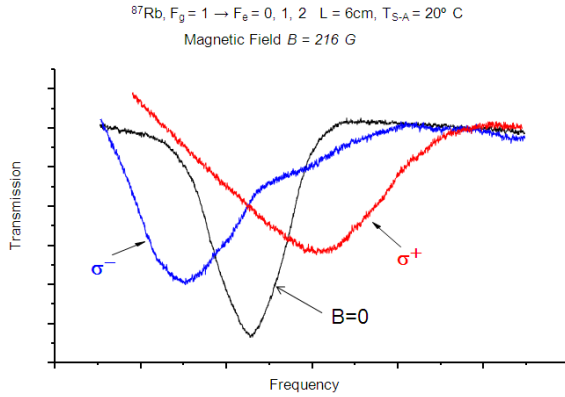


Fig. 1 Spectra of transmission in an ordinary cell for ^{87}Rb in the case $B = 0$ and $B = 200$ G for the radiations with polarisation σ^+ and σ^- .

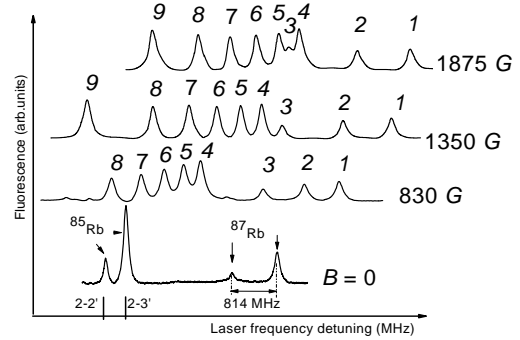


Fig. 2 Spectra of fluorescence in a NC for ^{85}Rb and ^{87}Rb for four values of B from 0 G to 1875 G.

In what follows, we will summarize the theoretical ingredients used to study the effect of an external magnetic field on the atomic transitions. Shifts of the Zeeman components and intensity of the corresponding transitions will be examined. Numerical applications to Rb and Na vapors confined in submicron thin vapor cell of thickness $L = \lambda/2$ are compared with experimental results.

2. EXPERIMENTAL PART

Sketch of the experimental setup is presented in Fig.3a. The circularly polarized light of extended cavity diode laser (ECDL, $\lambda = 780$ nm, $P_L \sim 30$ mW, $\gamma_L < 1$ MHz) resonant with ^{87}Rb D_2 transition frequency, after passing through Faraday isolator is directed onto the Rb NC 2 with the thickness of vapor column $L = \lambda/2$, at an angle close to normal.

The needed temperature regime of the NC ($T_{SA} \sim 110 - 120$ °C, $T_W \sim 140 - 150$ °C, corresponding to $N \sim 6 \times 10^{12} - 1.5 \times 10^{13}$ atoms/cm 3) is provided by a special oven with 3 openings: 2 inlets for laser beam passage and one orthogonal inlet for side fluorescence detection. This geometry allows simultaneous recording of fluorescence and transmission spectra. The fluorescence signal is detected by a photodiode 4 with an aperture of 1 cm 2 which is placed at 90° angle of the laser propagation direction. The photodiode signal is recorded by a digital four channel storage oscilloscope, Tektronix TDS 2014B.

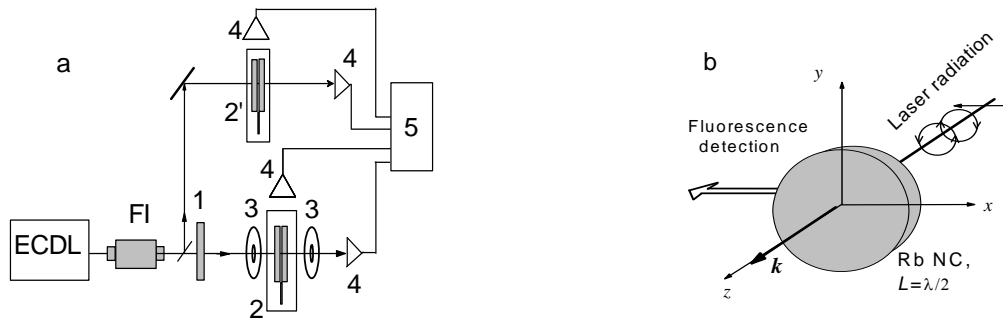


Fig.3 a - Sketch of the experimental setup. FI - Faraday isolator, 1 - $\lambda/4$ plate, 2 - STC and the oven, 2' - the auxiliary NC and the oven, 3 - RMs, 4 - photodetectors, 5 - digital storage oscilloscope; b - mutual orientations of laser excitation and detection of fluorescence emitted by a NC of $L = \lambda/2$.

A Glan prism is used to purify initial linear radiation polarization of the laser radiation; to produce a circular polarization a $\lambda/4$ plate 1 is utilized. The geometrical configuration of the experiment is shown in Fig.3b. Magnetic field is directed along the laser radiation propagation direction \mathbf{k} ($\mathbf{B} \parallel \mathbf{k}$).

With the help of a beam splitter, 50% of the pump beam is directed on the auxiliary 2' NC with Rb used as a frequency reference for $B = 0$. In some cases the reference spectrum is transmission spectrum¹² obtained with an auxiliary NC of thickness $L = \lambda$. The longitudinal magnetic field is applied to the NC by a system of Helmholtz coils (not shown in Fig.3a). The B -field strength is measured by a calibrated Hall gauge. Among the advantages of this setup is the possibility to apply strong magnetic field using widely available strong permanent magnets (PM). In spite of strong inhomogeneity of B -field, due to small thickness of the atomic vapor column inside NC ($L = 390$ nm) the variation of B inside the column is less than 0.1 G, i.e. by several orders less than the applied B value.

3. THEORETICAL BACKGROUND AND NUMERICAL CALCULATIONS

The so-called Dirac equation⁸ for an electron to order v^2/c^2 is the starting point to study the spectra of an atom within an electromagnetic field describes by the potentials $\{\vec{A}, V\}$:

$$\left[\frac{1}{2m} \left(\vec{p} + \frac{e}{c} \vec{A} \right)^2 + \frac{e}{mc} \vec{S} \cdot \vec{\nabla} \wedge \vec{A} - \frac{p^4}{8m^3 c^2} - \frac{e\hbar}{8m^2 c^2} \Delta V - \frac{e}{2m^2 c^2} \vec{S} \cdot (\vec{\nabla} V \wedge \vec{p}) - eV \right] \Psi = E\Psi \quad (2)$$

with $\vec{S} = \frac{\hbar}{2} \vec{\sigma}$ where $\vec{\sigma} = (\sigma_x, \sigma_y, \sigma_z)$, σ_i ($i = x, y, z$) are the matrices of Pauli. For a potential $V = V(r) = \frac{Ze}{r}$, the term $-\frac{e}{2m^2 c^2} \vec{S} \cdot (\vec{\nabla} V \wedge \vec{p})$ describing the spin-orbit interaction is rewritten on a more compact

form $H_{SO} = \xi(r) \vec{L} \cdot \vec{S}$. It is worth to notice that this term leads naturally to calculate the Hamiltonian matrix in the basis $|n, L, J, F, m_F\rangle \equiv |F, m_F\rangle$ with $\vec{F} = \vec{I} + \vec{J}$ and $\vec{J} = \vec{L} + \vec{S}$. Thus for the Zeeman interaction, defined by $H_Z = -\vec{\mu}_L \cdot \vec{B} - \vec{\mu}_S \cdot \vec{B} - \vec{\mu}_I \cdot \vec{B}$ with $\vec{\mu}_L = -\frac{\beta}{\hbar} \vec{L}$ the magnetic orbital momentum, $\vec{\mu}_S = -\frac{2\beta}{\hbar} \vec{S}$ the magnetic moment of spin \vec{S} and $\vec{\mu}_I = -\frac{g_I \beta}{\hbar} \vec{I}$ the magnetic moment of the nuclear spin \vec{I} where $\beta = \frac{e\hbar}{2mc}$ is the Bohr

magneton, the basis $|F, m_F\rangle$ can be chosen as a good basis to the first order if the condition $E_Z \ll E_{SO}$ is fulfilled. For the magnetic field that we apply to the nano-cells, this condition is respected as the magnetic field will vary from 0 to 10^4 G. One should note that all the previous discussion is valid for a magnetic field \vec{B} supposed uniform ($\vec{A} = \frac{1}{2} (\vec{B} \wedge \vec{r})$), which is what we have supposed in the development of the Zeeman interaction. Although interaction of atoms with laser radiation field in such cells is strictly anisotropic, however due to nanometric longitudinal size of the NCs, one may consider this hypothesis of uniformity as valid. This assumption is conformed by numerical calculation for inhomogeneity of B -field 150 G/mm.

The Hamiltonian of interaction $H_Z = -\vec{\mu}_L \cdot \vec{B} - \vec{\mu}_S \cdot \vec{B} - \vec{\mu}_I \cdot \vec{B}$ may be expanded using different forms¹⁰⁻¹⁴, we chose a formulation¹⁰ which leads to

$$H_Z = \left(-\frac{\mu_B}{\hbar} \right) \vec{B} \cdot (\vec{L} + g_S \vec{S} + g_I \vec{I}) \quad (3)$$

where g_S , g_I are respectively the spin and the nuclear Landé factor.

We adopt a matrix representation in the coupled basis, that is, the basis of the unperturbed atomic state vectors $|n=3, L, J, F, m_F\rangle \equiv |F, m_F\rangle$ to evaluate the matrix elements of the Hamiltonian (3). In this basis, the diagonal matrix elements are given by

$$\langle F, m_F | H | F, m_F \rangle = E_0(F) + \mu_B g_F m_F B_Z \quad (4)$$

where $E_0(F)$ is the initial energy¹⁵ of the sublevel $|F, m_F\rangle$ and g_F is the effective Landé factor¹⁵.

Non-zero off-diagonal matrix elements verify the selection rules $\Delta L = \Delta J = \Delta m_F = 0$, $\Delta F = \pm 1$ and are given by

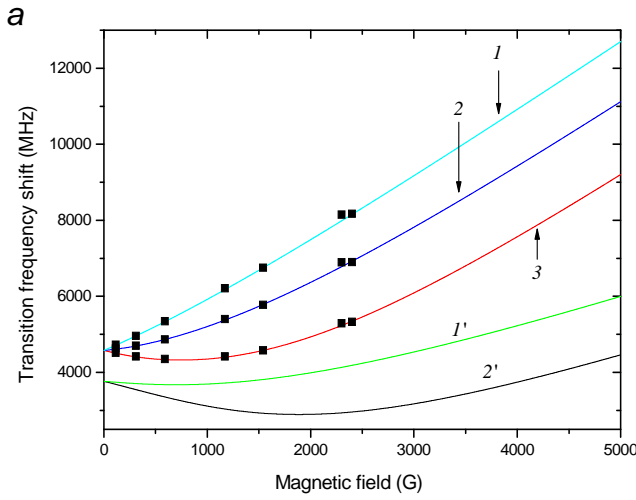


Fig. 4a Transition frequency shift versus magnetic field for ^{87}Rb , D_1 line

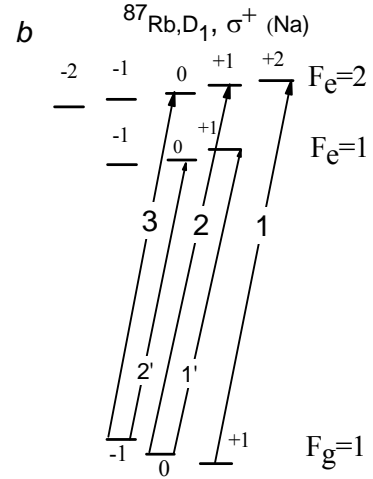


Fig. 4b Diagram of the labels $1, 2, 3$ and $1', 2'$

$$\begin{aligned} \langle F-1, m_F | H | F, m_F \rangle &= \langle F, m_F | H | F-1, m_F \rangle = -\frac{\mu_B B_Z}{2} (g_J - g_I) \\ &\times \left(\frac{[(J+I+1)^2 - F^2][F^2 - (J-I)^2]}{F} \right)^{1/2} \left(\frac{F^2 - m_F^2}{F(2F+1)(2F-1)} \right)^{1/2} \end{aligned} \quad (5)$$

The Hamiltonian matrix is then block diagonal where each block corresponds to a given value of m_F . The diagonalization of the Hamiltonian matrix allows one to find the eigenvectors and the eigenvalues, that is to determine the eigenvalues corresponding to the energies of Zeeman sublevels and the new states vectors which can be expressed in terms of the initial unperturbed atomic state vectors,

$$|\Psi(F'_g, m_{F'_g})\rangle = \sum_{F_g=3/2-J_g}^{F_g=3/2+J_g} \alpha_{F'_g F_g}^g(B_z, m_{F'_g}) |F_g, m_{F_g}\rangle \quad \text{and} \quad |\Psi(F'_e, m_{F'_e})\rangle = \sum_{F_e=3/2-J_e}^{F_e=3/2+J_e} \alpha_{F'_e F_e}^e(B_z, m_{F'_e}) |F_e, m_{F_e}\rangle \quad (6)$$

The state vectors $|F_e, m_e\rangle$ and $|F_g, m_g\rangle$ are the unperturbed state vectors, respectively, for the excited and the ground states. The coefficients $\alpha_{F'_e F_e}^e(B_z, m_{F'_e})$ and $\alpha_{F'_g F_g}^g(B_z, m_{F'_g})$ are mixing coefficients, respectively, for the excited and the ground states; they depend on the field strength and magnetic quantum numbers m_e or m_g .

In figure 4a we present the energy levels obtained by the Hamiltonian matrix diagonalization for D_1 line of ^{87}Rb atom. Figure 4b simply gives the definition of the notation used to label the transitions in Fig. 4a.

The transition frequency shift values are obtained on a quasi continuous variation of the B field intensity as we diagonalize 50 000 matrices. From low B field intensity to high B field variation, this diagonalization procedure allows us to follow exactly the eigenvalues by analyzing precisely the jump of the eigenvectors using a standard derivative analysis method. One should note that Fig. 4a shows the observed frequency shift, measured experimentally (which are obtained from Fig.2) while simultaneously on the same curves have been superposed the calculated ones. As previously written, the hypothesis of locally homogeneous and uniform magnetic field is verified.

The probability of a transition, induced by the interaction of the atomic electric dipole and the oscillating laser electric field is proportional to the spontaneous emission rate of the associated transition A_{e_g} , that is, to the square of the transfer coefficients modified by the presence of the magnetic field

$$\frac{8\pi^2}{3\varepsilon_0\hbar\lambda_{eg}^3} \left| \langle e | D_q | g \rangle \right|^2 = A_{eg} \propto a^2 \left[\Psi(F'_e, m_{F'_e}); \Psi(F'_g, m_{F'_g}); q \right] \quad (7)$$

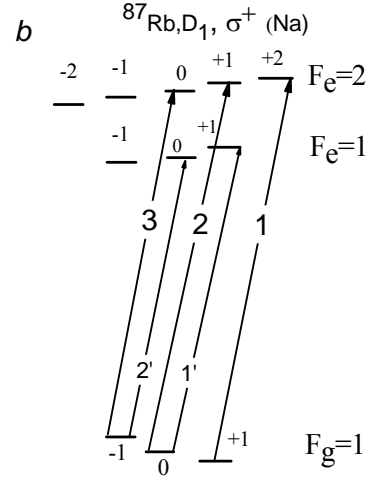
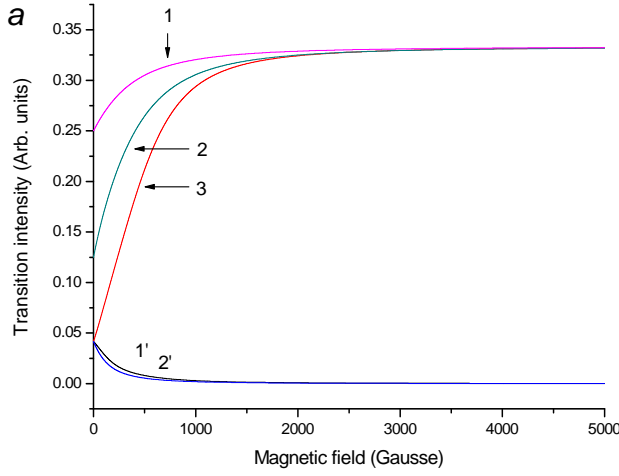


Fig.5a D_1 Line intensities for Na, transitions $F_g = 1 \rightarrow F_e = 1, 2$

Fig.5b Diagram of the labels 1, 2, 3 and 1', 2'

where D_q ($q = -1, 0, 1$) denote the standard components of the electric dipole moment $\vec{D} \cdot \vec{e} = \sum_q D_q e_q$.

In eq. (7), the transfer coefficients are expressed as

$$a \left[\Psi(F'_e, m_{F'_e}); \Psi(F'_g, m_{F'_g}); q \right] = \sum_{F_e, F_g} \alpha_{F'_e, F_e}^e(B_z, m_{F'_e}) a(F_e, m_{F_e}; F_g, m_{F_g}; q) \alpha_{F'_g, F_g}^g(B_z, m_{F'_g}), \quad (8)$$

where the unperturbed transfer coefficients have the following definition¹⁶

$$a(F_e, m_{F_e}; F_g, m_{F_g}; q) = (-1)^{1+I+J_e+F_e-F_g-m_{F_e}} \sqrt{(2J_e+1)(2F_e+1)(2F_g+1)} \begin{pmatrix} F_e & 1 & F_g \\ -m_{F_e} & q & m_{F_g} \end{pmatrix} \begin{Bmatrix} F_e & 1 & F_g \\ J_g & I & J_e \end{Bmatrix} \quad (9)$$

the parenthesis and curly brackets denote, respectively, the $3-j$ and $6-j$ symbols, g and e point respectively ground and excited states.

Figure 5a indicates clearly that the transition intensities versus the external magnetic field strength are strongly nonlinear for $B < 1500$ G. For higher values of B , at least to 5000 G, transitions 1, 2, 3 tend asymptotically to the same limit while transitions 1', 2' tend asymptotically to zero.

CONCLUSION

The $\lambda/2$ -Zeeman technique is shown to be a convenient and robust method for the study of individual transitions between the Zeeman sublevels of hyperfine levels in an external magnetic field. NC in external magnetic field allows exhibiting obviously the several Zeeman components due mainly to the suppression of the Doppler broadening. One of the goals of the construction of such an elegant tool was the possibility to remove this effect and it succeeds perfectly. As a result, the use of a NC as a nanomagnetometer seems a successful application of this device as it allows the measurement of extremely large gradient of magnetic field. Calculated and experimental results are in very good agreement.

Acknowledgement

The authors are grateful to A. Sarkisyan for his valuable participation in fabrication of the STC as well as to A. Papoyan for useful discussions. Research conducted in the scope of the International Associated Laboratory IRMAS. Armenian team thanks for a research grant PS 1868 from the Armenian National Science and Education Fund (ANSEF) based in New York, USA.

References

- [1] D. Sarkisyan, D. Bloch, A. Papoyan and M. Ducloy, "Sub-Doppler spectroscopy by sub-micron thin Cs vapour layer", *Opt. Commun.* **200**, 201 - 208 (2001).
- [2] G. Dutier, A. Yarovitski, S. Saltiel, A. Papoyan, D. Sarkisyan, D. Bloch and M. Ducloy, "Collapse and revival of a Dicke-type coherent narrowing in a sub-micron thick vapor cell transmission spectroscopy", *Europhys. Lett.* **63** (1), 35 - 41 (2003).
- [3] D. Sarkisyan, T. Becker, A. Papoyan, P. Thoumany and H. Walther, "Sub-Doppler Fluorescence on atomic D₂ line of Sub-Micron Rubidium Vapor Layer", *Appl. Phys. B* **76**, N6, pp. 625 - 631 (2003).
- [4] D. Sarkisyan, T. Varzhapetyan, A. Sarkisyan, Yu. Malakyan, A. Papoyan, A. Lezama, D. Bloch and M. Ducloy, "Spectroscopy in an extremely thin vapor cell: Comparing the cell-length dependence in fluorescence and in absorption techniques", *Phys. Rev. A* **69**, 065802 (4p.) (2004).
- [5] A. Papoyan, D. Sarkisyan, K. Blush, M. Auzinsh, D. Bloch and M. Ducloy, "Magnetic field-induced mixing of hyperfine states of the Cs 6P level observed with a submicron vapor cell", *Laser Physics* **13**, 1467 - 1477 (2003).
- [6] D. Sarkisyan, A. Papoyan, T. Varzhapetyan, K. Blush and M. Auzinsh, "Hyperfine structure Zeeman effect on of an atomic D₁ line of a sub-micron ⁸⁷Rb vapor layer", *Opt. and Spectrosc.* **96**, 328 - 334 (2004).
- [7] D. Sarkisyan, A. Papoyan, T. Varzhapetyan, K. Blush and M. Auzinsh, "Fluorescence of rubidium in a submicrometer vapor cell: spectral resolution of atomic transitions between Zeeman sublevels in a moderate magnetic field", *J. Opt. Soc. Am. B* **22**, 88 - 95 (2005).
- [8] M. Weissbluth, *Atoms and Molecules*. Academic, New-York (1978) and references herein.
- [9] A. Sargsyan, G. Hakhumyan, A. Papoyan, D. Sarkisyan, A. Atvars and M. Auzinsh, "A novel approach to quantitative spectroscopy of atoms in a magnetic field and applications based on an atomic vapor cell with $L = \lambda$ ", *Appl. Phys. Lett.* **93**, 021119 (3p.) (2008).
- [10] P. Tremblay, A. Nichaud, M. Levesque, S. Theriault, M. Breton, J. Beaubien, and N. Cyr, "Absorption profiles of alkali-metal D lines in the presence of a static magnetic field," *Phys. Rev. A* **42**, 2766 (1990).
- [11] E. B. Aleksandrov, M. P. Chaika, and G. I. Khvostenko, *Interference of Atomic States* (Springer-Verlag, New York, 1993).
- [12] V. Papoyan, D. H. Sarkisyan, K. Blush, M. Auzinsh, D. Bloch, and M. Ducloy, "Magnetic Field-Induced Mixing of the Cs 6²P_{3/2} Level Observed with a Submicron Vapor Cell", *Laser Physics* **13**, 1-11 (2003).
- [13] B. W. Shore, *The Theory of Coherent Atomic Excitation, Multilevel Atoms and Incoherence* (Wiley Interscience, New York, 1990).
- [14] D. Sarkisyan, A. Papoyan, T. Vazhapetyan, J. Alnis, K. Blush and M. Auzinsh, "Sub-Doppler spectroscopy of Rb atoms in a sub-micron vapour cell in the presence of a magnetic field", *J. Opt. A: Pure Appl. Opt.* **6**, S142-S150 (2004).
- [15] Daniel A. Steck, "Sodium D Line Data," available online at <http://steck.us/alkalidata> (revision 2.1.3, 26 August 2009).
- [16] E. de Clercq, M. de Labachellerie, G. Avila, P. Cerez and M. Tetu, "Laser diode optically pumped caesium beam," *J. Phys. France* **45**, 239-247 (1984).